AIP | Applied Physics Letters

# Square optical vortices generated by binary spiral zone plates

Nan Gao, Changqing Xie, Chun Li, Chunshui Jin, and Ming Liu

Citation: Appl. Phys. Lett. **98**, 151106 (2011); doi: 10.1063/1.3581044
View online: http://dx.doi.org/10.1063/1.3581044
View Table of Contents: http://apl.aip.org/resource/1/APPLAB/v98/i15
Published by the American Institute of Physics.

# Square optical vortices generated by binary spiral zone plates

Nan Gao,[1] Changqing Xie,[1,a)] Chun Li,[2] Chunshui Jin,[2] and Ming Liu[1]
[1]*Key Laboratory of Microelectronics Devices and Integrated Technology, Institute of Microelectronics, Chinese Academy of Sciences, Beijing 100029, People's Republic of China*
[2]*State Key Lab of Applied Optics, Changchun Institute of Optics, Fine Mechanics and Physics, Chinese Academy of Sciences, Changchun 130033, People's Republic of China*

(Received 22 February 2011; accepted 30 March 2011; published online 12 April 2011)

Binary phase square spiral zone plates (BPSSZPs), a special type of binary phase vortex lenses, are introduced to generate focused optical vortices showing square symmetry. The numerical solution and fabrication method, as well as the experimental results are given. Different from conventional vortex lenses, these BPSSZPs produce focused vortices with small topological charge following a modulo-4 transmutation rule. In addition, the central diffracted image rotates in the vicinity of the focal plane. These interesting properties suggest that BPSSZPs might become key components for many potential applications such as optical image processing and quantum computation. © *2011 American Institute of Physics*. [doi:10.1063/1.3581044]

Optical vortex, also known as phase singularity, has aroused considerable interest in recent years due to its unique physical properties and promising applications.[1–5] To date, various diffractive optical elements (DOEs) of producing optical vortices with circular symmetry, such as spiral phase plates (SPPs),[6,7] spiral zone plates (SZPs),[8] spiral photon sieves,[9] fractal zone plates,[10] Devil's vortex lenses,[11] or q plates,[12] have been reported.

However, for certain practical applications, square symmetry is preferred in the far field. For example, square symmetry is needed in precision alignment of accelerator[13] and optical alignment of two near plates.[14] In addition, square DOEs are better suited to the intrinsic geometry of an array of rectangular pixels.[15] Recently, square Fresnel zone plates with spiral phase[16] have been proposed. Similar to SPPs and Devil's vortex lenses, this kind of zone plates suffer from continuous phase profile, which are often approximated as multilevel staircase structures. Specialized manufacturing techniques, such as multimask-and-etch method, gray-level mask lithography, or direct writing process with varied exposure dosages must be employed. Even with precise process control, owing to the spatial sampling, quantization error is inevitable.

In this letter, we propose a type of binary phase square SZPs (BPSSZPs) to generate focused optical vortices with square symmetry, and we report the design, fabrication, experimental demonstration, and performance analysis of BPSSZPs. The binary phase profile can be realized using standard planar process, thus reducing the fabrication complexity, which brings the expectation of cheaper DOEs production. Moreover, the central diffraction field of BPSSZPs exhibits low vortex charges following a modulo-4 transmutation rule,[17] and rotates in the vicinity of the focal plane, which were not discussed in the previous publication.[16] These interesting features could enable BPSSZPs for numerous potential applications.

Figures 1(a)–1(d) illustrates the geometry of BPSSZPs with different topological charges, where the white areas correspond to 0 phase delay, and the black ones represent $\pi$ phase delay. A BPSSZP's transmittance function $t_{\mathrm{BPSSZP}}$ is expressed as a binarization of a spiral square lens $t_{\mathrm{SSL}}$ as follows:

$$t_{\mathrm{BPSSZP}}(r,\theta) = \mathrm{Bin}[t_{\mathrm{SSL}}(r,\theta)] = \mathrm{Bin}\{\exp[-ik\max(x^2,y^2)/2f]\exp(iP\theta)\} \quad (1)$$

with the following binarization function:

$$\mathrm{Bin}(t) = \begin{cases} 1 & \text{if} \quad \mathrm{Im}(t) > 0 \\ -1 & \text{if} \quad \mathrm{Im}(t) < 0 \end{cases},$$

where $k = 2\pi/\lambda$ is the wave number of incident light, $\lambda$ is the wavelength, $f$ is the focal length, $P$ is the topological charge of the BPSSZP, $(r,\theta)$ is the polar coordinate, and $(x,y)$ is the Cartesian coordinate.

From this transmittance function, one can analytically derive the diffraction intensity along the optical axis. Here we consider a BPSSZP illuminated by a normally incident plane wave. Using Fresnel diffraction formula, the axial intensity should be

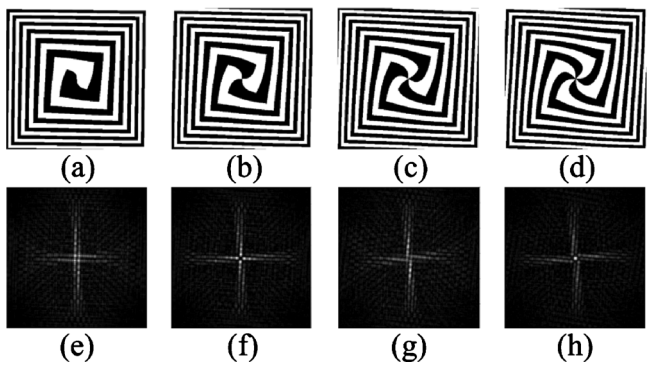


FIG. 1. BPSSZPs with different topological charge and their simulated diffraction image in the focal plane. [(a) and (e)] corresponds to $P=1$ BPSSZP, [(b) and (f)] to $P=2$, [(c) and (g)] to $P=3$, and [(d) and (h)] to $P=4$. In the simulation, the wavelength of incident light is 355 nm, and the focal length is 1.5 cm. The total simulation area is 512 $\mu$m × 512 $\mu$m.

a)Author to whom correspondence should be addressed. Electronic mail: xiechangqing@ime.ac.cn.

 

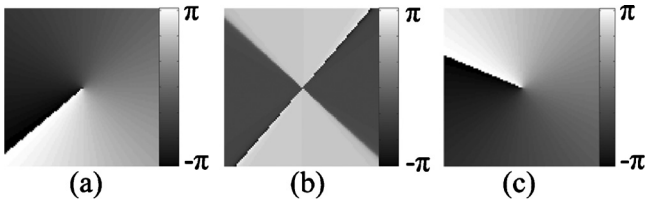


FIG. 2. Phase profile near the center vortex core in the focal plane of (a) $P=1$, (b) $P=2$, and (c) $P=3$ BPSSZPs. The total simulation area is 1 $\mu$m $\times 1$ $\mu$m.

$$I(z) = \left| (-iA/\lambda z) \int\int_s t_{\mathrm{BPSSZP}}(x,y)\exp(ik\sqrt{x^2+y^2+z^2})dxdy \right|^2 = \left| (-iA/\lambda z) \int\int_s t_{\mathrm{BPSSZP}}(r,\theta)\exp(ik\sqrt{r^2+z^2})rdrd\theta \right|^2, \quad (2)$$

where $z$ is the distance between the BPSSZP and the observation point, $A$ is the amplitude of the incident wave.

When $P$ is an odd integer, denoted as $P=2l+1$, $(l=0,\pm1,\pm2,\ldots)$, according to Eq. (1), $t_{\mathrm{BPSSZP}}(r,\theta+\pi)$ and $t_{\mathrm{BPSSZP}}(r,\theta)$ always keep a phase difference of $\pi$. As a result, the integral in Eq. (2) cancels out and $I(z)=0$, which reveals that optical vortex is generated along the optical axis. When $P$ is an even integer in the form of $P=2(2l+1)$, $(l=0,\pm1,\pm2,\ldots)$, $t_{\mathrm{BPSSZP}}(r,\theta+\pi/2)$ and $t_{\mathrm{BPSSZP}}(r,\theta)$ will keep a $\pi$ phase difference, thus the integral in Eq. (2) also cancels out and makes $I(z)$ zero. However, when $P$ is an even integer taking the form $P=4l$, $(l=0,\pm1,\pm2,\ldots)$ since $\max[r^2\sin^2(\theta+\pi/4), r^2\cos^2(\theta+\pi/4)] \neq \max(r^2\sin^2\theta, r^2\cos^2\theta)$ in Eq. (1), the integral in Eq. (2) cannot be canceled out and $I(z)$ is no long zero in general.

To further investigate the focusing behavior of BPSSZPs, numerical simulations based on Fresnel diffraction formula are performed. The wavelength of incident light is 355 nm, and the focal length is 1.5 cm. As can be seen in Figs. 1(e)–1(g), as $P=1$, 2, or 3, the focal pattern is characterized by a square dark core with crossed bright arms and four bright spots. When $P=4$, as predicted above, the axial intensity is nonzero, instead, a single bright spot is generated at the center [Fig. 1(h)].

To better understand the vortex nature of the diffraction field, phase profile near the focal spot is also calculated and illustrated in Fig. 2. When $P=1$ [Fig. 2(a)], the phase distribution exhibits a spiral structure and increases $2\pi$ every loop around the center, which reveals a +1 topological charge. Figure 2(b) corresponds to a $P=2$ BPSSZP. As expected, it presents a phase singularity with topological charge of +2. What is striking is that when $P=3$, as shown in Fig. 2(c), the vortex charge is $-1$, instead of its expected value of +3. Further simulations indicate that the topological charge always keeps to be 0, $\pm1$, or $\pm2$, when $P$ is an arbitrary integer, following a modulo-4 transmutation rule (Table I).[17] This phenomenon originates from the intrinsic fourfold rotational symmetry of the BPSSZP (Ref. 17) and instability of vortices under the background perturbation.[2,18] BPSSZPs thus provide convenient implementation of canonical vortex transmutation without nonlinear material, and can be utilized as a modulo-4 operation for the orbital angular momentum states, which should find its applications in quantum computation.[5,19] In addition, since any continuous azimuthal profile can be decomposed into a series of vortex components through Fourier expansion, a BPSSZP can thus act as a filter, which converts all the high-order vortex components to low-order ones in the focal plane. This conversion might be very useful in the optical image processing, where slow azimuthal variations are needed.[20]

TABLE I. Topological charge of BPSSZP and the center vortex core in the focal plane.

| Topological charge of BPSSZP | Topological charge of the focal vortex |
|---|---|
| $P=0,\pm4,\pm8,\pm12,\ldots$ | 0 |
| $P=\pm1,\pm5,\pm9,\pm13,\ldots$ | $\pm1$ |
| $P=\pm2,\pm6,\pm10,\pm14,\ldots$ | $\pm2$ |
| $P=\pm3,\pm7,\pm11,\pm15,\ldots$ | $\mp1$ |

Using standard planar process, a $P=1$ BPSSZP with focal length of 20 cm and total structure area of 24 mm $\times 24$ mm was obtained. The fabrication steps are as follow: (1) making a mask with an electron beam mask writer (MEBES4700S) donated by Applied Materials company. (2) Coating a layer of positive photoresist (Shipley S9920) onto a fused silica substrate. (3) Transferring the mask pattern to the photoresist layer by using photolithography. (4) Transferring the photoresist pattern onto the fused silica substrate by inductively coupled plasma etching. By controlling the etching time, the fused silica is etched to a depth of 370 nm, which gives a $\pi$ phase shift for 355 nm incident light. (5) Removing the photoresist layer. After the BPSSZP was manufactured as shown in Figs. 3(a) and 3(b), a testing system shown in Fig. 3(c) was used to evaluate the performance of the BPSSZP. The incident laser beam is focused by a microscopy objective and passes through a pinhole filter. Then, the incident light source impinges on a BPSSZP after a

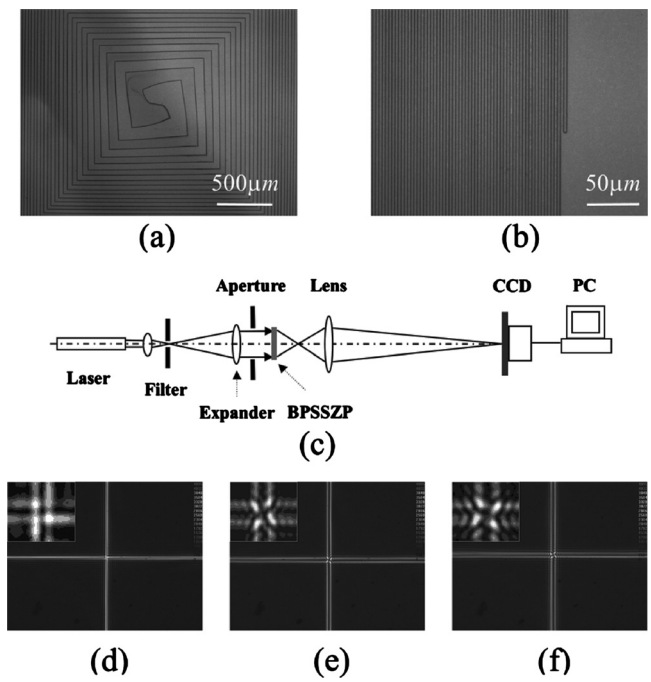


FIG. 3. Experimental results. (a) $\times 50$ microscopy image of our $P=1$ BPSSZP near the center. (b) $\times 500$ microscopy image of the BPSSZP near the outermost zones. (c) Experimental system for optical demonstration of a BESSZP. Diffraction patterns of the BPSSZP are imaged by CCD at (d) z =f, (e) z=0.997f, and (f) z=1.003f.

collimating lens and an aperture. A diffraction pattern is generated at the focal plane of BPSSZP, and then magnified by 8 times by a zoom lens and finally recorded by a charge coupled device (CCD) camera. Figure 3(d) is the diffraction pattern in the focal plane, displaying the same profile predicted by numerical simulations [Fig. 1(e)]. This good agreement between numerical simulation and experimental result verifies the BPSSZP's ability to generate focused vortex beam with square symmetry. To further study the defocus property, diffraction patterns at $z=0.997f$ [Fig. 3(e)] and $z=1.003f$ [Fig. 3(f)] are also recorded. It is interesting that the center dark core remains while the four bight spots rotate around the central core and the spacing between the two parallel arms scales. Similar to the propagation-invariant beams that have a rotating PSF,[21] the rotation feature of BPSSZP can be applied in depth estimation[22] and auto focusing systems. Comparing with the $4f$ system proposed in Ref. 22, BPSSZP should be particularly useful when a compact system is preferred, owing to its focusing ability. Furthermore, when square symmetry is needed in the system, BPSSZP is undoubtedly a better choice.

In summary, BPSSZPs that can produce focused optical vortices with unique features has been introduced. Both numerical and experimental results have verified the superior BPSSZPs' properties. Not only suitable to conventional applications of optical vortex such as particle manipulation when square symmetry are needed but this kind of DOEs should also be of great value in various applications including optical image processing, depth estimation, auto focusing, and quantum computation.

The authors acknowledge the support of National Basic Research Program of China and the National Outstanding Youth Foundation of China (Grants Nos. 2007CB935302 and 60676008).

[1]L. Allen, M. W. Beijersbergen, R. J. C. Spreeuw, and J. P. Woerdman, Phys. Rev. A **45**, 8185 (1992).
[2]M. S. Soskin, V. N. Gorshkov, and M. V. Vasnetsov, Phys. Rev. A **56**, 4064 (1997).
[3]L. Paterson, M. P. MacDonald, J. Arlt, W. Sibbett, P. E. Bryant, and K. Dholakia, Science **292**, 912 (2001).
[4]D. G. Grier, Nature (London) **424**, 810 (2003).
[5]A. Mair, A. Vaziri, G. Weihs, and A. Zeilinger, Nature (London) **412**, 313 (2001).
[6]M. W. Beijersbergen, R. P. C. Coerwinkel, M. Kristensen, and J. P. Woerdman, Opt. Commun. **112**, 321 (1994).
[7]W. C. Cheong, W. M. Lee, X.-C. Yuan, L.-S. Zhang, K. Dholakia, and H. Wang, Appl. Phys. Lett. **85**, 5784 (2004).
[8]N. R. Heckenberg, R. McDuff, C. P. Smith, and A. G. White, Opt. Lett. **17**, 221 (1992).
[9]C. Xie, X. Zhu, L. Shi, and M. Liu, Opt. Lett. **35**, 1765 (2010).
[10]S. H. Tao, X. C. Yuan, J. Lin, and R. E. Burge, Appl. Phys. Lett. **89**, 031105 (2006).
[11]W. D. Furlan, F. Gimenez, A. Calatayud, and J. A. Monsoriu, Opt. Express **17**, 21891 (2009).
[12]L. Marrucci, C. Manzo, and D. Paparo, Phys. Rev. Lett. **96**, 163905 (2006).
[13]W. B. Herrmannsfeldt, M. J. Lee, J. J. Spranza, and K. R. Trigger, Appl. Opt. **7**, 995 (1968).
[14]B. Fay, J. Trotel, and A. Frichet, U.S. Patent No. 4,311,389 (19 January 1982).
[15]F. J. González, J. Alda, B. Ilic, and G. D. Boreman, Appl. Opt. **43**, 6067 (2004).
[16]B. Zhang and D. Zhao, Opt. Lett. **35**, 1488 (2010).
[17]A. Ferrando, M. Zacares, M. Garcia-March, J. A. Monsoriu, and P. F. de Cordoba, Phys. Rev. Lett. **95**, 123901 (2005).
[18]G. Molina-Terriza, J. Recolons, J. P. Torres, L. Torner, and E. M. Wright, Phys. Rev. Lett. **87**, 023902 (2001).
[19]J. Leach, M. J. Padgett, S. M. Barnett, S. Franke-Arnold, and J. Courtial, Phys. Rev. Lett. **88**, 257901 (2002).
[20]M. Clampin, J. E. Krist, D. R. Ardila, D. A. Golimowski, G. F. Hartig, H. C. Ford, G. D. Illingworth, F. Bartko, N. Benítez, J. P. Blakeslee, R. J. Bouwens, T. J. Broadhurst, R. A. Brown, C. J. Burrows, E. S. Cheng, N. J. G. Cross, P. D. Feldman, M. Franx, C. Gronwall, L. Infante, R. A. Kimble, M. P. Lesser, A. R. Martel, F. Menanteau, G. R. Meurer, G. K. Miley, M. Postman, P. Rosati, M. Sirianni, W. B. Sparks, H. D. Tran, Z. I. Tsvetanov, R. L. White, and W. Zheng, Astrophys. J. **126**, 385 (2003).
[21]R. Piestun, Y. Y. Schechner, and J. Shamir, J. Opt. Soc. Am. A **17**, 294 (2000).
[22]A. Greengard, Y. Y. Schechner, and R. Piestun, Opt. Lett. **31**, 181 (2006).